

# Protective Effect of Electro-Acupuncture on Neural Myelin Sheaths Mediated through Activation of Epidermal Growth Factor Receptor after Compressed Spinal Cord Injury

Rui Gong<sup>1</sup>, Shanquan Sun<sup>1\*</sup>, Qi Zhao<sup>1</sup>, Yuan Zhong<sup>1</sup>, Haijun Yu<sup>1</sup>, Lan Ma<sup>1</sup>, Shiye Xu<sup>1</sup>, Wei Zhang<sup>1</sup>, Kejie Mou<sup>2</sup> and Jun Xue<sup>2</sup>

<sup>1</sup>Institute of Neuroscience, Chongqing Medical University, No.1 Medical College Road, Yuzhong District, Chongqing, 400016, China

<sup>2</sup>Department of Neurosurgery, Bishan Hospital of the First Affiliated Hospital of Chongqing Medical University, No.82 New Street Biqian Street, Bishan District, Chongqing, 402760, China

## Abstract

Electro acupuncture has been widely used to treat demyelinating diseases, such as multiple sclerosis (MS), acute haemorrhagic leukoencephalitis (AHLE), compressed spinal cord injury (CSCI). However, the protective effect of electro acupuncture (EA) on neural myelin sheaths remains controversy attributed to the dimness of its therapeutic mechanism. In this study, we tried to explore the protective mechanism of EA in a custom-designed model of CSCI. Zusanli (ST36) and Huantiao (GB30) acupoints were stimulated by EA. The motor functions were monitored by Basso, Beattie and Bresnahan locomotor rating scale. The pathological changes in axonal myelinated fibers were estimated by luxol fast blue (LFB) and transmission electron microscopy (TEM). Epidermal growth factor receptor (EGFR), oligodendrocyte transcription factor 2 (Olig2), caspase-3 and phosphorylated Akt1 (pAkt1) were detected by immunofluorescence and western blot assays. After 7-day treatment of EA, the expression of p-EGFR, pAkt1 and Olig2 was significantly up-regulated which was consistent with changes of locomotor skill and ultrastructure of myelin sheath. By contrast, the expression of active caspase-3 was obviously down-regulated. Our results indicated that the protective effect of EA on neural myelin sheaths might be mediated via activation of EGFR after CSCI.

**Keywords:** Electro-acupuncture; Compressed spinal cord injury; Remyelination, p-EGFR; pAkt1; Olig2; Caspase-3

## Introduction

Electro acupuncture is a form of acupuncture where a small electric current is passed between pairs of acupuncture needles. It can not only augment the use of regular acupuncture, but also introduce electric current into human body. By promoting oligodendrocyte proliferation and differentiation, electro acupuncture (EA) has been widely used in demyelinating diseases and showed excellent curative effect [1-4]. However, the mechanism of EA is largely unknown.

Compressed spinal cord injury (CSCI), which is caused by a metastatic extramedullary tumor, lumbar intervertebral disc herniation, has become a global issue. Previous studies have proved that extensive demyelination induced by oligodendrocytes apoptosis was the major pathological change after CSCI [5-7], suggesting that the main goal in treatment of CSCI is the protection of oligodendrocytes. Epidermal growth factor receptor (EGFR, also known as erbB1 or HER-1), the member of the epidermal growth factor family (EGF-family), is vital for the proliferation and differentiation of OPCs [8-12]. After combined with its specific ligands, intrinsic intracellular protein-tyrosine kinase of EGFR auto-phosphorylated [13,14] and p-EGFR activated Akt1 [15,16]. pAkt1 can not only up-regulate the expression of oligodendrocyte transcription factor (Olig2) [17], which plays critical and positive roles in the generation of OPCs [18-20], but also down-regulate the expression of caspase-3 that contributes to the apoptosis of OPCs [21-23]. Hence, we supposed that the protective effect of electro acupuncture on neural myelin sheaths after compressed spinal cord injury is mediated through activation of EGFR and its downstream proteins. However, this hypothesis should be certified by experiments.

Through observing before and after the treatment two groups of neurological function, the numbers and ultrastructure of axonal myelinated fibers, the expression of p-EGFR, pAkt1, Olig2 and caspase-3 circumference variations, we tried to elucidate the protective mechanism of EA on neural myelin sheaths in CSCI.

## Materials and Methods

A total of 90 Sprague-Dawley (SD) rats weighing 250 g to 320 g

were randomly divided into nine groups: normal groups (neither do compression spinal cord injury nor EA stimulation, EA groups (receiving electro acupuncture stimulation after decompression surgery) and control groups (without receiving electro acupuncture stimulation after decompression surgery) for 1 day after decompression, EA and control groups for 7 days after decompression, EA and control groups for 14 days after decompression, EA and control groups for 21 days after decompression (n=10/group). All rats were provided by the Experimental Animal Center of Chongqing Medical University. All experimental procedures were performed in accordance with the Animal Care and Ethics Committee and were approved by the Ministry of Science and Technology of the People's Republic of China. The rats were housed in a 26°C room on a 12:12 dark/light cycle and were given enough food and water.

## Surgical procedure

The model of compressed spinal cord injury (CSCI) was referred to the method designed by our team [24]. The rats were anesthetized with the intraperitoneal injection of 3.5% chloral hydrate and were subsequently fixed on a surgical table lying on back. The laminectomy was performed at L1 to expose the spinal cord, and the processed anterior and posterior arthrosis was excised without damaging the spinal cord. A custom-made device for chronic compressed spinal cord injury was immobilized the exposed dorsal surface of the spinal cord.

**\*Corresponding author:** Shanquan Sun, Institute of Neuroscience, Chongqing Medical University, No.1 Medical College Road, Yuzhong District, Chongqing, 400016, China, Tel: +86 23 68485555; Fax: +86 23 68485868; E-mail: [sunsq2151@cqmu.edu.cn](mailto:sunsq2151@cqmu.edu.cn), [sunsq2151@sohu.com](mailto:sunsq2151@sohu.com)

**Received** September 08, 2016; **Accepted** September 19, 2016; **Published** September 21, 2016

**Citation:** Gong R, Sun S, Zhao Q, Zhong Y, Yu H, et al. (2016) Protective Effect of Electro-Acupuncture on Neural Myelin Sheaths Mediated through Activation of Epidermal Growth Factor Receptor after Compressed Spinal Cord Injury. J Spine 5: 332. doi: [10.4172/2165-7939.1000332](https://doi.org/10.4172/2165-7939.1000332)

**Copyright:** © 2016 Gong R, et al. This is an open-access article distributed under the terms of the Creative Commons Attribution License, which permits unrestricted use, distribution, and reproduction in any medium, provided the original author and source are credited.

After sutured, the nuts were exposed out of the skin. Motor, sensory, bowel and bladder functions were completely regular after woke up. From the first day after surgery, the screw was screwed into 1/4 turn (about 0.25 mm), and then twisted every 3-4 days until the double lower limb paralysis, incontinence (approximately 20 days. It is regarded as a successful model and the rats were then decompressed.

### Electro acupuncture

For the EA group, electro acupuncture treatment was deducted from the first day of decompression until sacrifice. All EA was given at 9:00 a.m. to 11:00 a.m. every day. The rats were fastened for 30 min during EA administration without anesthetization [25] (Because of complete paralysis of hind limbs, the mouse can't touch in the stimulation). In this study, we selected Zusanli (ST36) and Huantiao (GB30) acu-points to treat rats with CSCI based on two considerations. Firstly, these two acu-points are able to speed up the conduction of nerve impulses. Secondly, they are the two essential acu-points for the treatment of CSCI, prescribed by the Classics of the Traditional Chinese Medicine (TCM1). After cleaning the skin with alcohol, a pair of needle was connected with the output terminals of an EA apparatus (Model SDZ-II, Suzhou HuaTuo Medical Instrument Co., Ltd, Suzhou, China). Dense-spare frequencies (60 Hz for 1.05 s and 2 Hz for 2.85 s, alternatively) were used for EA [26] and the intensity of the stimulation was applied for 30 min at 2 mA. Animals in control groups didn't receive any treatment.

### Neurological function assessment

Locomotor activity was examined based on Basso, Beattie, and Bresnahan (BBB) rating scale in an open field, according to indications of published articles by two independent observers in a double-blind manner [27-29]. A total of 21 scores from 0 (complete paralysis) to 21 (normal) were recorded after decompression of CSCI at 1<sup>st</sup>, 7<sup>th</sup>, 14<sup>th</sup> and 21<sup>st</sup> days.

### Luxol fast blue

Mice were humanely euthanized and spinal cord were removed and fixed in 4% paraformaldehyde for 24 hours at 4°C. Sections from the center of the injury were selected along with sections from 0.5 cm to 0.7 cm rostral and caudal to the injury site. The tissues were then dehydrated successively in 10%, 20% and 30% sucrose solution, and embedded in optimal cutting temperature (OCT) compound. Ten micrometer thick (10 µm) transverse sections of the spinal cord were manufactured on a frozen slicer. Spinal cord sections were stained with Luxol fast blue at 60°C for 2 h. Sections were then rinsed in 95% ethanol and differentiated in 0.05% Lithium carbonate solution followed by 70% ethanol. Differentiation was stopped by distilled water until unmyelinated tissue turned white. Twelve random micrographs from the lateral funiculus were obtained under an Olympus microscope with an objective lens of 40x. At least 10 randomly sections were captured. These micrographs were further measured the total number of myelinated fibers using Image-J software (National Institutes of Health, USA) by a blinded investigator.

### TEM observation

Specimen from the sections perfused with 4% paraformaldehyde was fixed in 2.5% glutaraldehyde for 2 days, and then successively fixed in 2% osmic acid for 1h and dehydrated in serial alcohol and propylene oxide. After dehydration, specimen was embedded in araldite for morphometric analyses on semi thin sections. Ultrathin sections mounted on copper grids were stained with uranyl acetate and lead citrate. Twelve random images with a magnification of 15000× from the lateral funiculus were obtained using a transmission electron

microscopy (TEM; Hitachi-7500, Hitachi Ltd., Tokyo, Japan). These images were analyzed using the MIAS image analysis system to determine the ratio of myelin thickness to axon diameter (G-ratio) [30].

### Double-labeling immunofluorescence

To identify p-EGFR, pAkt1, caspase-3, Olig2 and NG2+ (the marker of oligodendrocyte precursor cells) co-expression in the spinal cord sections, we used the primary antibodies listed in Table 1. Tissue sections were rewarmed, rinsed and incubated in 5% donkey serum (Jackson Immuno Research, Lancaster, PA, USA) for 1 h at 37°C in a humidified atmosphere to permeabilise the tissue and block non-specific protein-protein interactions. The tissues were then incubated with the primary antibody overnight at +4°C. These tissue sections were rinsed again with 0.01mol/L PBS. The secondary antibody (red) was cy3 conjugated goat anti-rabbit IgG (H+L) used at a 1/200 dilution for 1.5h at 37°C in a humidified atmosphere in the dark. Alexafluor 488 goat anti-mouse IgG (H+L) used to label NG2 (green) at a 1/200 dilution for 1.5 h at 37°C in a humidified atmosphere in the dark. Nuclear dye (4',6-diamidino-2-phenylindole, 1:20; Bestbio Inc., China) was used to stain the cell nuclei (blue) for 5 min. The tissue sections were then washed and mounted in 50% glycerol dissolved in PBS. The samples were observed under a confocal microscope (Leica TCS SP2, Germany). All the digital images from lateral funiculus were captured in a double-blind manner from four random fields per section of the injured epicenter of the cross sections in the rats. The number of p-EGFR+-NG2, pAkt1+-NG2, Olig2+-NG2 and caspase-3+-NG2 per field was counted for analysis.

### Western blot

Tissues soaked at 4°C in buffer containing 50 mmol/L ethylenediaminetetraacetic acid, 2 µg/mL of leupeptin, 2 µg/mL of pepstatin A, 2 mmol/L phenyl methyl sulfonyl fluoride, and 200 KIE/mL aprotinin were broken down mechanically using a blender. The homogenates were then centrifuged at 10,000×g for 20 min at 4°C. The supernatant was collected, and protein concentration was determined using a Bradford assay kit (Bio-Rad, Hercules, CA, USA). The proteins of the sample were separated using 10% SDS-PAGE and then transferred to poly vinylidenedifluoride membrane. Blotted membranes were incubated in 5% skim milk to block non-specific protein-protein interactions. For immunoblotting, the following primary antibodies were used: the polyclonal rabbit anti-olig2 antibody (1:1000; Abcam, Cambridge, UK, ab81093); the polyclonal rabbit anti-Akt1 antibody (1:1000; Abcam, Cambridge, UK, ab66138); the monoclonal rabbit anti-EGFR antibody (1:1000; Abcam, Cambridge, UK, ab52894); and the polyclonal rabbit anti-caspase3 antibody (1:1000; Abcam, Cambridge, UK, ab44976). The secondary antibodies were used alkaline phosphatase-conjugated anti-IgG antibodies (1:10000, Santa Cruz). Immuno reactive bands were visualized using

Antibody name	Manufacturer	Dilution	Host	Labelling
Anti-EGFR antibody ( ab15669)	Abcam, USA	1:200	rabbits	Epidermal growth factor receptor
Anti-pAkt1 antibody (ab66138)	Abcam, USA	1:200	rabbits	pAkt1
Anti-olig2 antibody (ab81093)	Abcam, USA	1:200	rabbits	Oligodendrocyte transcription factor 2
Anti-active caspase-3 antibody (ab13847)	Abcam, USA	1:200	rabbits	Active caspase-3
Anti-NG2 antibody (ab50009)	Abcam, USA	1:200	mouse	NG2

**Table 1:** Antibodies used in immune-fluorescence and western blot in this study.

a chemiluminescent substrate (Pierce Inc., Rockford, IL, USA). Western bands were quantified by gel densitometry (Bio-Rad). A ratio of protein-beta-actin for each sample was obtained (each point was repeated in triplicate).

## Statistical Analysis

Statistical analyses were performed using GraphPad Prism 5.0 (GraphPad Software, Inc., USA). Differences between control groups and EA groups were compared using two independent samples t-test. Correlation between phosphor-EGFR and pAkt-1, Olig2, caspase-3 was then analyzed with Pearson correlation.  $P < 0.05$  was considered statistically significant.

## Results

### Neurological function assessment

To evaluate the effect of EA on functional recovery, we assessed the locomotor skills in an open field using the Basso, Beattie, and Bresnahan (BBB) rating scale. Two independent samples t-test was performed: No statistically significant differences were found between control groups and EA groups at day 1 and day 7 (EA for 1 day group vs. control for 1 day group,  $p > 0.05$ ; EA for 7 days group vs. control for 7 days group,  $p > 0.05$ ; Figure 1); while the mean BBB scores in EA groups for 14 days and 21 days were remarkably increased when compared with its corresponding groups in control group (EA for 14 days group vs. control for 14 days group,  $p < 0.01$ ; EA for 21 days group vs. control for 21 days group,  $p < 0.01$ , Figure 1). The results suggested that EA could protect the neurological function if we have enough time.

### Demyelination after CSCI

Myelinated nerve fibers were investigated using luxol fast blue (LFB) and the number of myelinated nerve fibers was counted by Image J (National Institutes of Health, USA). Statistical analysis showed that no statistically significant differences were found between the control and EA groups at 1<sup>st</sup> day and 7<sup>th</sup> day (EA for 1-day group vs. control for 1-day group,  $p > 0.05$ ; EA for 7-day group vs. control for 7-day group,  $p > 0.05$ , Figure 2). However, the number of myelinated nerve fibers in EA groups for 14<sup>th</sup> and 21<sup>st</sup> day was remarkably increased when compared with its corresponding groups in control group (EA for 14 days vs. control for 14 days,  $p < 0.05$ ; EA for 21 days vs. control for 21 days,  $p < 0.05$ , Figure 2). These results suggested that EA have a protective effect on neural myelin sheaths.

### Ultra-structural results

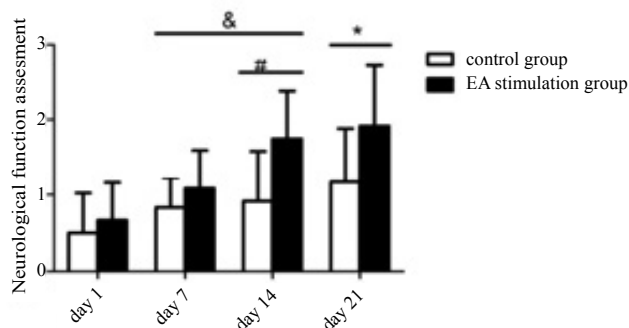
We then investigated the ultrastructural features of myelinated nerve fiber at the lateral funiculus in the white matter by transmission electron microscope (TEM). The result showed that axons had a varied swelling degree and cell organelles in the axoplasm became degenerative and lost both in control and EA groups, and the layers of myelin sheaths became disordered, thickened and even broken down after CSCI (Figure 2). However, the swelling degree of myelin sheaths in EA groups for 14<sup>th</sup> day was milder than those in control groups and the layers of myelin sheaths in EA groups for 14<sup>th</sup> day were more compact than those in the control groups (Figure 2).

### Expression of p-EGFR and pAkt1

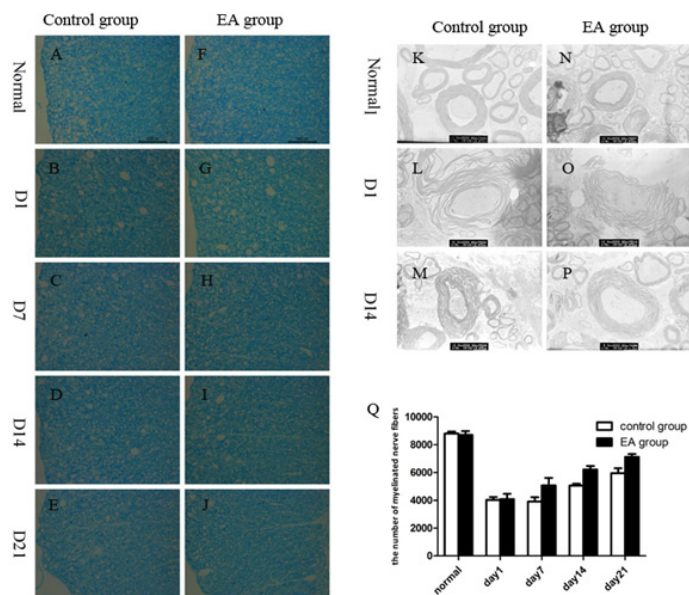
The p-EGFR+NG2 and pAkt1+NG2 cells in the spinal cord sections were identified by double-labeling immunofluorescence and the expression of p-EGFR and pAkt1 was detected by western blot, using antibodies against NG2, p-EGFR and pAkt1. Double-labeling immunofluorescence results showed that: the p-EGFR+NG2 and pAkt1+NG2 cells was increased and reached the maximum on 14<sup>th</sup> day both in control and EA groups (Figures 3B-3E and Figures 4B-4E); the p-EGFR+NG2 and pAkt1+NG2 cells were distributed sparsely in control groups but widely in EA groups for 14<sup>th</sup> day (Figures 3C-3E and Figures 4C-4E); a positive correlation was also found between the number of p-EGFR+NG2 and pAkt1+NG2 cells (Not displayed in the picture). The western blot results showed that: compared with control group, the expression of p-EGFR and pAkt1 in EA groups for 7<sup>th</sup>, 14<sup>th</sup> and 21<sup>st</sup> day was significantly increased (Figures 3F-3H, EA for 14<sup>th</sup> day vs. control for 14<sup>th</sup> day,  $p < 0.05$ ; EA for 7<sup>th</sup> day vs. control for 7<sup>th</sup> day,  $p < 0.05$ ; EA for 21<sup>st</sup> day vs. control for 21<sup>st</sup> day,  $p < 0.05$ . Figures 4F-4H, EA for 14<sup>th</sup> day vs. control for 14<sup>th</sup> day,  $p < 0.05$ ; EA for 7<sup>th</sup> day vs. control for 7<sup>th</sup> day,  $p < 0.05$ ; EA for 21<sup>st</sup> day vs. control for 21<sup>st</sup> day,  $p < 0.05$ ).

### Expression of Olig2 involved in OPCs proliferation/differentiation

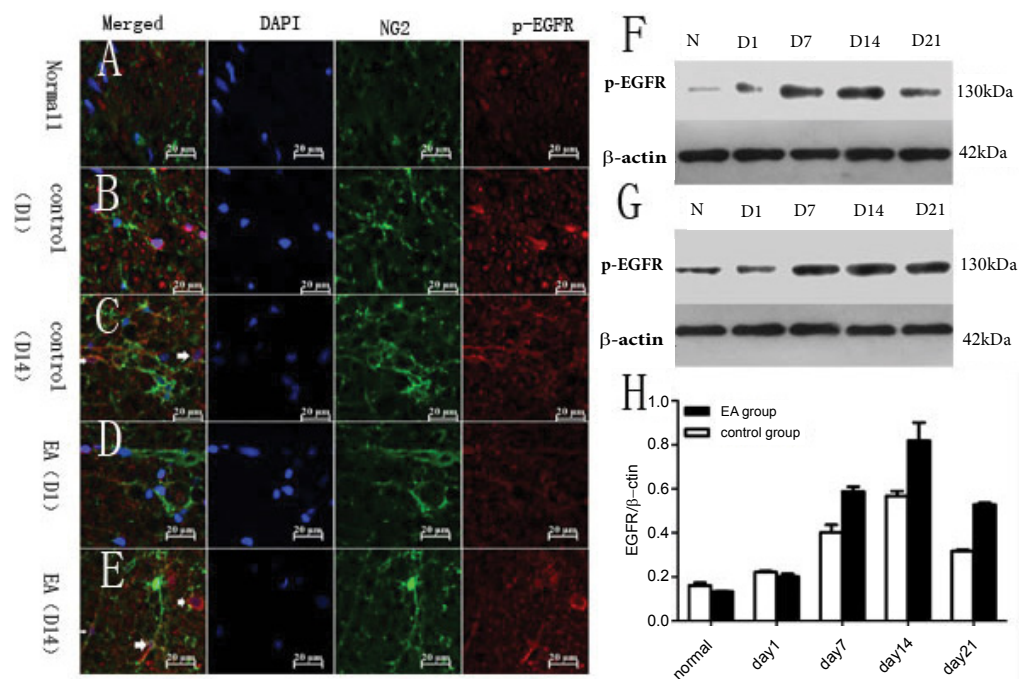
To further explore the protective mechanism of electro acupuncture, we examined Olig2 which is participated in oligodendrogenesis [31-34] and can be regulated by pAkt117. Double-labeling immunofluorescence results showed that: The Olig2+NG2 cells was increased and reached the maximum on 14<sup>th</sup> day in control groups (Figures 5B-5E); the Olig2+NG2 cells were distributed sparsely



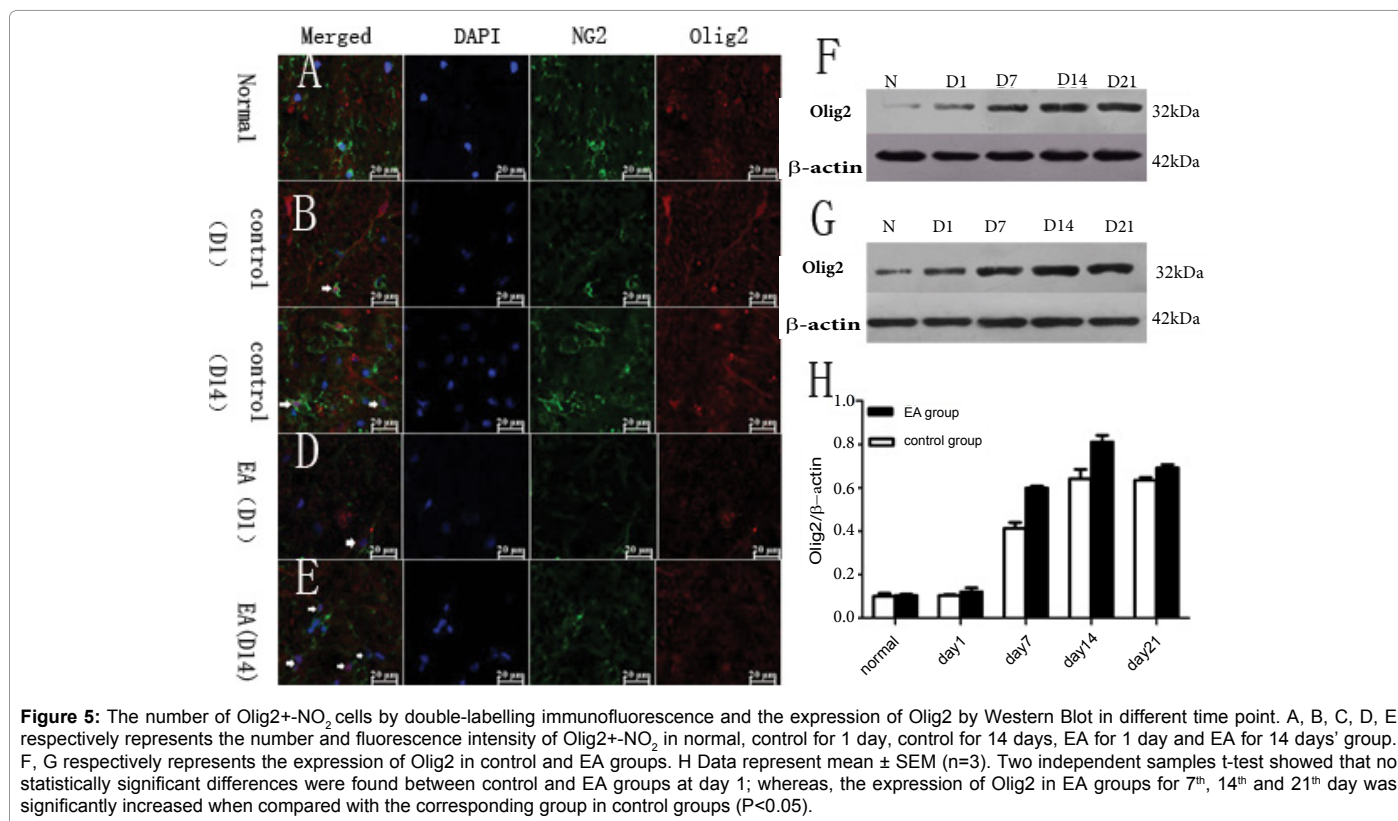
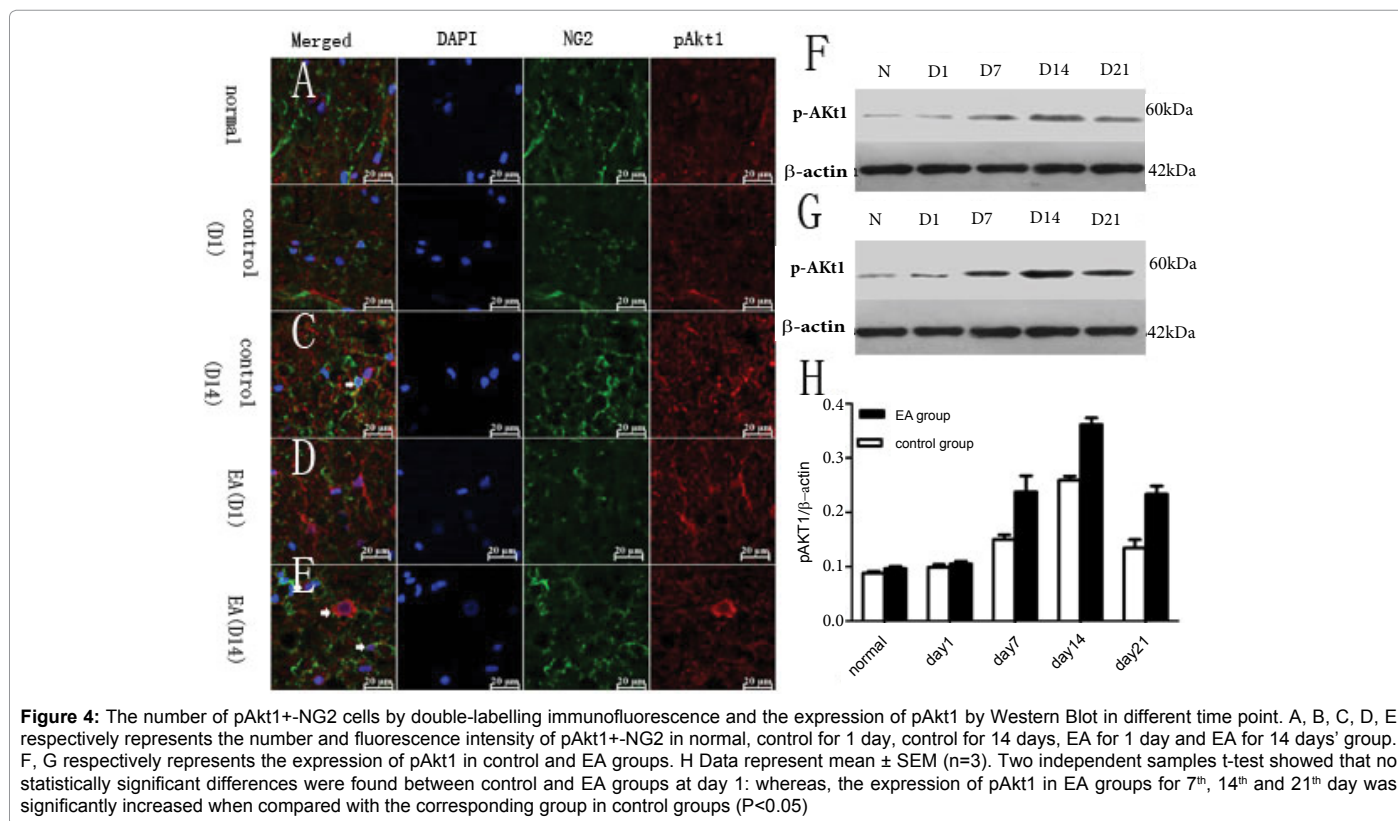
**Figure 1:** Neurological function assessment. Locomotor scores were assessed based on the Basso, Beattie, and Bresnahan (BBB) rating scale. Data represent mean  $\pm$  SE (2, 10 per group). One-way ANOVA performed that the mean BBB scores of rats in control and EA stimulation groups were increased with time. The BBB scores in control groups for 14 days were remarkably increased when compared with control for 1<sup>st</sup> day and the BBB scores of rats in EA for 14 days were remarkably increased when compared with EA for 1, 7 days ( $P < 0.01$ ). Two independent samples t-test was then performed that: no statistically significant differences were found between control and EA stimulation groups at baseline and day 7; while the mean BBB scores in EA stimulation group for 14 days and 21 days were remarkably increased when compared with its corresponding groups in control group. 1:  $P < 0.01$  compared with the control for 14 days' group,  $p < 0.01$  compared with the control for 21 days group; and  $p < 0.01$  compared with EA for 7 days group.

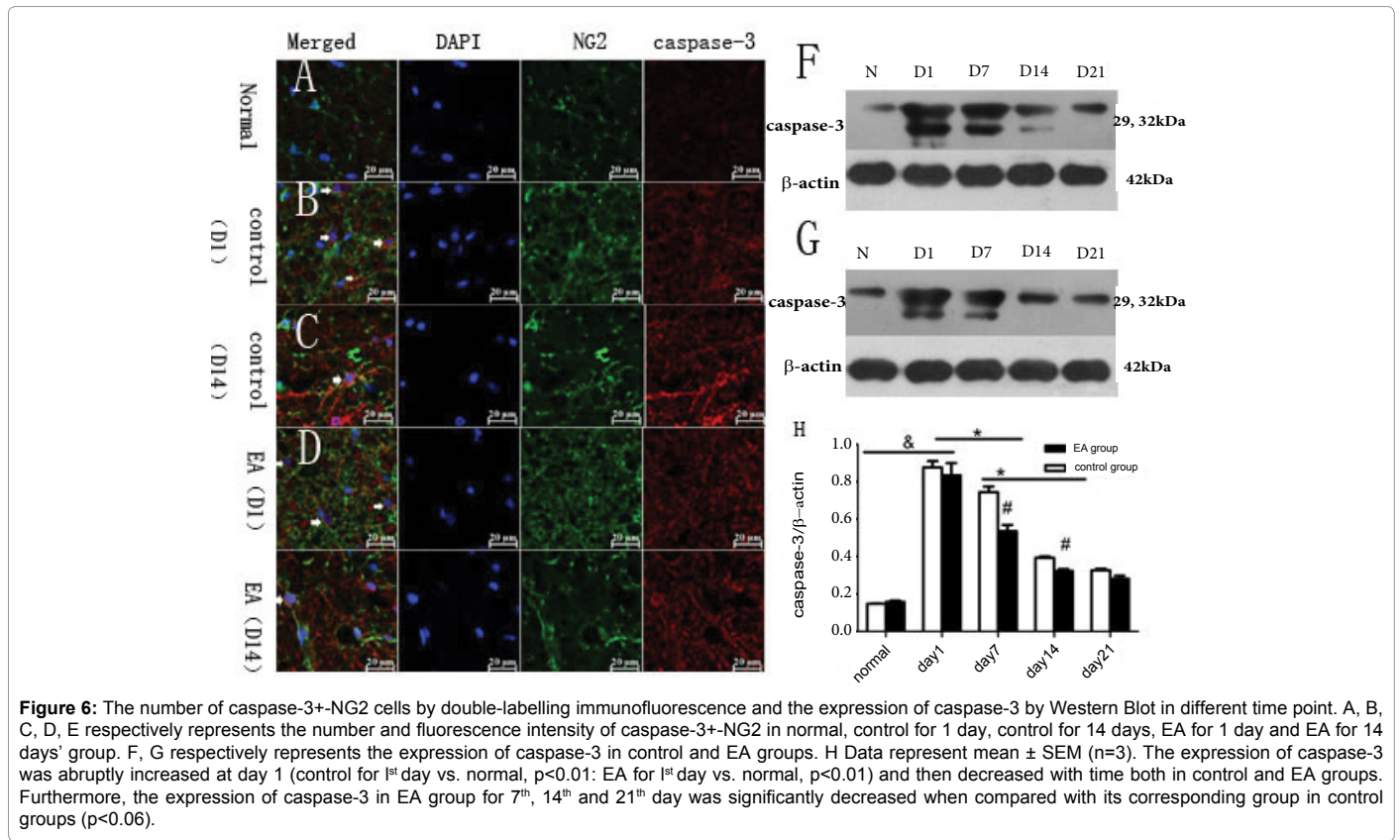


**Figure 2:** The pathological changes in myelinated nerve fibers at the lateral funiculus in the white matter were detected by luxol fast blue and transmission electron microscopy (TEM). (A-E) The myelinated nerve fibers at the lateral funiculus in the white matter in control groups, scale bar: 25 mm. (F-J) The myelinated nerve fibers at the lateral funiculus in the white matter in EA groups, scale bar: 25 mm. (K-N) Extensively distributed myelinated fibers in normal groups were routinely observed and the myelinated axons showed a normal axoplasm with well-preserved cellular structure. (L,Q) The axons both in control and EA groups for 1<sup>st</sup> day varied swollen. myelin sheaths became edema; the layer of myelin sheaths became disorder, thick and even broken down. (M) The swollen degree of myelin sheaths in control groups for 14<sup>th</sup> day was milder than that in control groups for 1<sup>st</sup> day but never return normal. (P) The swollen degree of myelin sheaths in EA groups for 14<sup>th</sup> day was milder than that in EA groups for 1<sup>st</sup> day and in control groups for 14<sup>th</sup> day. (Q) The number of myelinated axons at the corresponding times both in control and EA groups. Compared with the normal groups, the number of myelinated nerve fibers was significantly decreased both in control and EA groups, and not returned to normal. No statistically significant differences were found between the control and EA groups for 1<sup>st</sup> day and 7<sup>th</sup> day ( $P > 0.05$ ). However, the number of myelinated nerve fibers in EA groups was remarkably increased compared with control groups for 14<sup>th</sup> and 21<sup>th</sup> day. (EA for 14 days group vs. control for 14 day group,  $P < 0.05$ ; EA for 21 days group vs. EA for 21 days group,  $P < 0.05$ ).



**Figure 3:** The number of p-EGFR+HG2 cells by double-labelling immunofluorescence and the expression of p-EGFR by Western Blot in different time point. A, B, C, D, E respectively represents the number and fluorescence intensity of p-EGFR+NG2 in normal, control for 1 day, control for 14 days, EA for 1 day and EA for 14 days' group. F, G respectively represents the expression of p-EGFR in control and EA groups. H Data represent mean  $\pm$  SEM (n=3). Two independent samples t-test showed that no statistically significant differences were found between control and EA groups at day 1; whereas, the expression of EGFR in EA groups for 7<sup>th</sup>, 14<sup>th</sup> and 21<sup>th</sup> day was significantly increased when compared with the corresponding group in control groups ( $P < 0.05$ ).





in control groups but widely in EA groups for 14<sup>th</sup> day (Figures 5C-5E); a positive correlation was also found between the number of pAkt1+NG2 and Olig2+NG2 cells (Not displayed in the picture). Western blot results showed that: the expression of Olig2 in EA groups for 7<sup>th</sup>, 14<sup>th</sup> and 21<sup>st</sup> day was significantly increased (Figure 5). EA for 14<sup>th</sup> day vs. control for 14<sup>th</sup> day,  $p < 0.05$ ; EA for 7<sup>th</sup> day vs. control for 7<sup>th</sup> day,  $p < 0.05$ ; EA for 21<sup>st</sup> day vs. control for 21<sup>st</sup> day,  $p < 0.05$ ) when compared with the corresponding group in control groups.

### Expression of caspase-3 involved in apoptosis

Caspase-3 has been shown to play central role in apoptosis pathways. Meanwhile, the expression of caspase-3 can be down-regulated by pAkt1. Therefore, we examined the expression of caspase-3. Double-labeling immunofluorescence results showed that: the caspase-3+NG2 cells was abruptly increased at day 1 and then decreased with time both in control and EA groups (Figures 6B-6E); caspase-3+NG2 cells were distributed widely in control groups but sparsely in EA groups for 14<sup>th</sup> day (Figures 6C-6E); a negative correlation was also found between the number of pAkt1+NG2 and caspase-3+NG2 cells (Not displayed in the picture). The western blot results showed that: the expression of caspase-3 was abruptly increased at day 1 (control for 1<sup>st</sup> day vs. normal,  $p < 0.01$ ; EA for 1<sup>st</sup> day vs. normal,  $p < 0.01$ ) and then decreased with time both in control and EA groups, but still higher than those in normal groups (control groups vs. normal groups,  $P < 0.05$ ; EA groups vs. normal groups,  $P < 0.05$ , Figure 6). Furthermore, the expression of caspase-3 in EA group for 7<sup>th</sup>, 14<sup>th</sup> and 21<sup>st</sup> day was significantly decreased when compared with its corresponding group in control groups (EA for 7<sup>th</sup> day vs. control for 7<sup>th</sup> day,  $p < 0.05$ ; EA for 14<sup>th</sup> day vs. control for 14<sup>th</sup> day,  $p < 0.05$ ; EA for 21<sup>st</sup> day vs. control for 21<sup>st</sup> day; Figures 6F-6H).

### Discussion

Previous studies reported that EA treatment can increase the number and differentiation of endogenous OPCs and remyelination in the demyelinated spinal cord, [33-35]. However, the specific mechanism of promoting the proliferation and differentiation of endogenous OPCs and remyelination is largely unknown. In addition, it is known that extensive demyelination induced by oligodendrocytes apoptosis was the major pathological change after CSCI1, [36,37]. Therefore, the independent designing CSCI model was developed to observe whether electroacupuncture could promote the proliferation and differentiation of OPCs, remyelination and functional recovery. After 7-day treatment of EA, the neurological function was significantly improved, consistent with the improved ultrastructural features and numbers of myelinated nerve fibers. This result is consistent with the previous studies, which further shows that electro acupuncture can promote the proliferation and differentiation of OPCs, myelin formation and neural function recovery.

In order to further explore the protective mechanism of electro acupuncture on neural myelin sheaths, we next investigated the expression of p-EGFR and its downstream protein—pAkt1. Significant studies have been reported that p-EGFR functions as a regulator in the oligodendrocyte lineage, including induction of survival and proliferation [33,36-38]. After activated by specific ligands, such as EGF or neuregulin, EGFR phosphorylated and bound with SH2 domains of pAkt1 [15,16], thereby regulating the expression of other proteins in the cell. In this study, we found that the expression of p-EGFR, pAkt1 in the EA groups was significantly increased and p-EGFR-NG2+, pAkt1-NG2+ were found widely in the white matter. These results are consistent with the changes of neurological function, ultrastructural features and numbers of myelinated nerve fibers. The result suggested

that p-EGFR, pAkt1 were clearly up-regulated by EA to improve the recovery of the injured spinal cord.

Akt1 is one of the members of the pAkt (Protein kinase B, PKB) family, which is a key signaling protein in the cellular pathways. It can not only up-regulate the expression of oligodendrocyte transcription factor (Olig2) [17], but also down-regulate caspases family [39,40]. Therefore, we have tested Olig2 and caspase-3 based on the test of pAkt1.

The formation of oligodendrocytes is triggered by an increased activity of bHLH factors, in which Olig2 coupled with an increase in pAkt1 activity [17]. Olig2 is a class of bHLH transcription factor that is specially expressed by Olig cells in a restricted domain of the spinal cord ventricular zone and sequentially generates oligodendrocytes [41]. Olig2 is excellent in positively controlling OPCs generation [42-44] and can strongly up-regulate the OPCs in demyelinating diseases to benefit neuronal repair [45]. In this study, we found that the expression of Olig2 in the EA groups was significantly increased and Olig2+NG2 cells were widely distributed in the white matter. Meanwhile, the increase of Olig2 is consistent with the up-regulation of pAkt1. The result suggested that Olig2 was clearly up-regulated by EA to promote the recovery of the injured spinal cord and this effect may be attributed to pAkt1.

Caspases are a family of protease enzymes playing essential roles in programmed cell death, in which Caspase-3 that mediated main apoptosis pathways, including death receptor pathway, mitochondrial pathway and endoplasmic reticulum stress (ER stress) pathway [46], has been shown to play a central role. Our result also revealed that the expression of caspase-3 was sudden increased after CSCI, suggesting that caspase-3 plays a vital role in apoptosis of oligodendrocytes after CSCI. Meanwhile, the expression of caspase-3 can be down-regulated by pAkt [47]. Hence, we next investigated the expression of caspase-3. In the current study, we found that the expression of caspase-3 in the EA groups was significantly decreased and caspase-3+NG2 cells were sparsely distributed in the white matter. And the expression of caspase-3 and pAkt1 was negatively correlated: when the expression of pAkt1 was increased, the expression of Caspase-3 was decreased, and vice versa. These results suggested that EA stimulation can prevent oligodendrocytes from apoptosis by down-regulating the expression of caspase-3 and this effect may be closely related to the up-regulation of pAkt1.

## Conclusion

This study showed that the protective effect of EA on neural myelin sheaths might be mediated via activation of EGFR and its downstream associated proteins after CSCI. This study can provide experimental basis for the clinical application of EA.

## Acknowledgements

This study was supported by the National Natural Science Foundation of China (Grant No. 81403466 and 81273870) and the Graduate Research and Innovation Project foundation of Chongqing (Grant No.40010200100410).

## Declaration of Rights

The authors state that there are no actual or potential conflicts of interests.

## Submission Declaration and Verification

The authors have not published or submitted the manuscript elsewhere.

## References

- Huang S, Tang C, Sun S, Cao W, Qi W, et al. (2015) Protective effect of

electro-acupuncture on neural myelin sheaths is mediated via promotion of oligodendrocyte proliferation and inhibition of oligodendrocyte death after compressed spinal cord injury. *Mol Neurobiol* 52: 1870-1881.

- Ding Y, Zhang RY, He B, Liu Z, Zhang K, et al. (2015) Combination of electroacupuncture and grafted mesenchymal stem cells overexpressing TrkC improves remyelination and function in demyelinated spinal cord of rats. *Sci Rep* 5: 9133.
- Huang SF, Ding Y, Ruan JW, Zhang W, Wu JL, et al. (2011) An experimental electro-acupuncture study in treatment of the rat demyelinated spinal cord injury induced by ethidium bromide. *Neurosci Res* 70: 294-304.
- Chu NN, Xia W, Yu P, Hu L, Zhang R, et al. (2008) Chronic morphine-induced neuronal morphological changes in the ventral tegmental area in rats are reversed by electro-acupuncture treatment. *Addiction biology* 13: 47-51.
- Emery E, Aldana P, Bunge MB, Puckett W, Srinivasan A, et al. (1998) Apoptosis after traumatic human spinal cord injury. *J Neurosurg* 89: 911-920.
- Huang SQ, Tang CL, Sun SQ, Yang C, Xu J, et al. (2014) Demyelination initiated by oligodendrocyte apoptosis through enhancing endoplasmic reticulum-mitochondria interactions and Id2 expression after compressed spinal cord injury in rats. *CNS Neurosci Ther* 20: 20-31.
- Myers KR, Liu G, Feng Y, Zheng JQ (2016) Oligodendroglial defects during quaking viable cerebellar development. *Dev Neurobiol* 76: 972-982.
- Aguirre A, Dupree JL, Mangin JM, Gallo V (2007) A functional role for EGFR signalling in myelination and remyelination. *Nat Neurosci* 10: 990-1002.
- Galvez-Contreras AY, Quinones-Hinojosa A, Gonzalez-Perez O (2013) The role of EGFR and ErbB family related proteins in the oligodendrocyte specification in germinal niches of the adult mammalian brain. *Frontiers in cellular neuroscience* 7: 258.
- Chong VZ, Webster MJ, Rothmond DA, Weickert CS (2008) Specific developmental reductions in subventricular zone ErbB1 and ErbB4 mRNA in the human brain. *Int J Dev Neurosci* 26: 791-803.
- Hu Q, Zhang L, Wen J, Wang S, Li M, et al. (2010) The EGF receptor-sox2-EGF receptor feedback loop positively regulates the self-renewal of neural precursor cells. *Stem Cells* 28: 279-286.
- Sinor-Anderson A, Lillien L (2011) Akt1 interacts with epidermal growth factor receptors and hedgehog signalling to increase stem/transit amplifying cells in the embryonic mouse cortex. *Dev Neurobiol* 71:759-71.
- Scaltriti M, Baselga J (2006) The epidermal growth factor receptor pathway: a model for targeted therapy. *Clin Cancer Res* 12: 5268-5272.
- Yarden Y, Sliwkowski MX (2001) Untangling the ErbB signalling network. *Nat Rev Mol Cell Biol* 2: 127-137.
- Ng HY, Ko JM, Yu VZ, Ip JC, Dai W, et al. (2016) DESC, a novel tumor suppressor, sensitizes cells to apoptosis by downregulating the EGFR/AKT pathway in oesophageal squamous cell carcinoma. *Int J Cancer* 138: 2940-2951.
- Zhu Z, Yu W, Fu X, Sun M, Wei Q, et al. (2015) Phosphorylated Akt1 is associated with poor prognosis in esophageal squamous cell carcinoma. *J Exp Clin Cancer Res* 34: 95.
- Hayakawa-Yano Y, Nishida K, Fukami S, Gotoh Y, Hirano T, et al. (2007) Epidermal growth factor signaling mediated by grb2 associated binder-1 is required for the spatiotemporally regulated proliferation of olig2-expressing progenitors in the embryonic spinal cord. *Stem Cells* 25: 1410-22.
- Fancy SP, Zhao C, Franklin RJ (2004) Increased expression of Nkx2.2 and Olig2 identifies reactive oligodendrocyte progenitor cells responding to demyelination in the adult CNS. *Mol Cell Neurosci* 27: 247-54.
- Sun T, Hafner BP, Kaing S, Kitada M, Ligon KL, et al. (2006) Evidence for motoneuron lineage-specific regulation of Olig2 in the vertebrate neural tube. *Dev Biol* 292: 152-164.
- Buffo A, Vosko MR, Erturk D, Hamann GF, Jucker M, et al. (2005) Expression pattern of the transcription factor Olig2 in response to brain injuries: implications for neuronal repair. *Proceedings of the National Academy of Sciences of the United States of America* 102: 18183-8.
- Chen LX, Ma SM, Zhang P, Fan ZC, Xiong M, et al. (2015) Neuroprotective effects of oligodendrocyte progenitor cell transplantation in premature rat brain following hypoxic-ischemic injury. *PLoS One* 10: e0115997.
- Porter AG, Jänicke RU (1999) Emerging roles of caspase-3 in apoptosis. *Cell Death Differ* 6: 99-104.

23. Gonzalez-Fernandez E, Sanchez-Gomez MV, Perez-Samartin A, Arellano RO, Matute C (2014) A3 Adenosine receptors mediate oligodendrocyte death and ischemic damage to optic nerve. *Glia* 62: 199-216.
24. Jian LY, Quan SS, Jian WK, Hua YW (2006) The establishment of chronic compressed spinal cord injury model in the rat. *Chinese Journal of Clinical Anatomy Vol* 24: 320-324.
25. Wang H, Pan Y, Xue B, Wang X, Zhao F, et al. (2011) The anti-oxidative effect of electro-acupuncture in a mouse model of Parkinson's disease. *PLoS One* 6: e19790.
26. Huang S, Tang C, Sun S, Cao W, Qi W, et al. (2014) Protective effect of electro-acupuncture on neural myelin sheaths is mediated via promotion of oligodendrocyte proliferation and inhibition of oligodendrocyte death after compressed spinal cord injury. *Molecular neurobiology*.
27. Basso DM, Beattie MS, Bresnahan JC (1995) A sensitive and reliable locomotor rating scale for open field testing in rats. *J Neurotrauma* 12: 1-21.
28. Lee-Kubli CA, Ingves M, Henry KW, Shiao R, Collyer E, et al. (2016) Analysis of the behavioral, cellular and molecular characteristics of pain in severe rodent spinal cord injury. *Experimental neurology* 278: 91-104.
29. Basso DM, Bresnahan JC (1996) Graded histological and locomotor outcomes after spinal cord contusion using the NYU weight-drop device versus transection. *Experimental Neurology* 139: 244-56.
30. Pavelko KD, Van Engelen BG, Rodriguez M (1998) Acceleration in the rate of CNS remyelination in lysolecithin-induced demyelination. *J Neurosci* 18: 2498-2505.
31. Jakovcevski I, Zecevic N (2005) Olig transcription factors are expressed in oligodendrocyte and neuronal cells in human fetal CNS. *J Neurosci* 25: 10064-10073.
32. Jakovcevski I, Zecevic N (2005) Sequence of oligodendrocyte development in the human fetal telencephalon. *Glia* 49: 480-491.
33. Gonzalez-Perez O, Quiñones-Hinojosa A (2010) Dose-dependent effect of EGF on migration and differentiation of adult subventricular zone astrocytes. *Glia* 58: 975-983.
34. Menn B, Garcia-Verdugo JM, Yaschine C, Gonzalez-Perez O, Rowitch D, et al. (2006) Origin of oligodendrocytes in the subventricular zone of the adult brain. *J Neurosci* 26: 7907-7918.
35. Ding Y, Yan Q, Ruan JW, Zhang YQ, Li WJ, et al. (2009) Electro-acupuncture promotes survival, differentiation of the bone marrow mesenchymal stem cells as well as functional recovery in the spinal cord-transected rats. *BMC neuroscience*. 10: 35.
36. Gonzalez-Perez O, Romero-Rodriguez R, Soriano-Navarro M, Garcia-Verdugo JM, Alvarez-Buylla A (2009) Epidermal growth factor induces the progeny of sub-ventricular zone type B cells to migrate and differentiate into oligodendrocytes. *Stem cells*. 27: 2032-43.
37. Ivkovic S, Canoll P, Goldman JE (2008) Constitutive EGFR signalling in oligodendrocyte progenitors leads to diffuse hyperplasia in postnatal white matter. *J Neurosci*. 28: 914-22.
38. Gonzalez-Perez O, Alvarez-Buylla A (2011) Oligodendrogenesis in the sub-ventricular zone and the role of epidermal growth factor. *Brain Res Rev* 67: 147-156.
39. Chen WS, Xu PZ, Gottlob K, Chen ML, Sokol K, et al. (2001) Growth retardation and increased apoptosis in mice with homozygous disruption of the Akt1 gene. *Genes Dev* 15: 2203-2208.
40. Rad SK, Kanthimathi MS, Abd Malek SN, Lee GS, Looi CY et al. (2015) Cinnamomum cassia Suppresses Caspase-9 through stimulation of Akt1 in MCF-7 cells but not in MDA-MB-231 cells. *PLoS One* 10: e0145216.
41. Lu QR, Yuk D, Alberta JA, Zhu Z, Pawlitzky I, et al. (2000) Sonic hedgehog-regulated oligodendrocyte lineage genes encoding bHLH proteins in the mammalian central nervous system. *Neuron*. 25: 317-29.
42. Nery S, Wichterle H, Fishell G (2001) Sonic hedge-hog contributes to oligodendrocyte specification in the mammalian forebrain. *Development* 128: 527-540.
43. Sun T, Echelard Y, Lu R, Yuk DI, Kaing S, et al. (2001) Olig bHLH proteins interact with homeodomain proteins to regulate cell fate acquisition in progenitors of the ventral neural tube. *Curr Biol* 11: 1413-1420.
44. Tsigelny IF, Mukthavaram R, Kouznetsova VL, Chao Y, Babic I, et al. (2015) Multiple spatially related pharmacophores define small molecule inhibitors of olig2 in glioblastoma. *Oncotarget*.
45. Cai J, Chen Y, Cai WH, Hurlock EC, Wu H, et al. (2007) A crucial role for Olig2 in white matter astrocyte development. *Development* 134: 1887-1899.
46. Zuo H, Lin T, Wang D, Peng R, Wang S, et al. (2014) Neural cell apoptosis induced by microwave exposure through mitochondria-dependent caspase-3 pathway. *Int J Med Sci*. 11: 426-35.
47. Flores AI, Mallon BS, Matsui T, Ogawa W, Rosenzweig A, et al. (2000) Akt-mediated survival of oligodendrocytes induced by neuregulins. *J Neurosci* 20: 7622-7630.